**ASMS**

Comprehensive Lipidome Analysis by Shotgun Lipidomics on a Hybrid Quadrupole-Orbitrap-Linear Ion Trap Mass Spectrometer

Reinaldo Almeida, Josch Konstantin Pauling, Elena Sokol, Hans Kristian Hannibal-Bach, Christer S. Ejsing

Department of Biochemistry and Molecular Biology, VILLUM Center for Bioanalytical Sciences University of Southern Denmark, 5230 Odense, Denmark
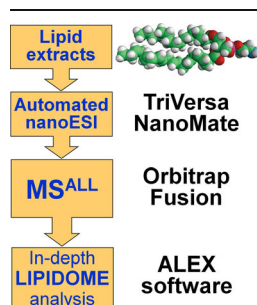
Abstract. Here we report on the application of a novel shotgun lipidomics platform featuring an Orbitrap Fusion mass spectrometer equipped with an automated nanoelectrospray ion source. To assess the performance of the platform for in-depth lipidome analysis, we evaluated various instrument parameters, including its high resolution power unsurpassed by any other contemporary Orbitrap instrumentation, its dynamic quantification range and its efficacy for in-depth structural characterization of molecular lipid species by quadrupole-based higher-energy collisional dissociation (HCD), and ion trap-based resonant-excitation collision-induced dissociation (CID). This evaluation demonstrated that FTMS analysis with a resolution setting of 450,000 allows distinguishing isotopes from different lipid species and features a linear dynamic quantification range of at least four orders of magnitude. Evaluation of fragmentation analysis demonstrated that combined use of HCD and CID yields complementary fragment ions of molecular lipid species. To support global lipidome analysis, we designed a method, termed MS^{ALL}, featuring high resolution FTMS analysis for lipid quantification, and $FTMS^2$ analysis using both HCD and CID and $ITMS^3$ analysis utilizing dual CID for in-depth structural characterization of molecular glycerophospholipid species. The performance of the MS^{ALL} method was benchmarked in a comparative analysis of mouse cerebellum and hippocampus. This analysis demonstrated extensive lipidome quantification covering 311 lipid species encompassing 20 lipid classes, and identification of 202 distinct molecular glycerophospholipid species when applying a novel high confidence filtering strategy. The work presented here validates the performance of the Orbitrap Fusion mass spectrometer for in-depth lipidome analysis.

Key words: Shotgun lipidomics, Hybrid quadrupole-Orbitrap-linear ion trap mass spectrometry, High mass resolution, Nanoelectrospray ionization, Collision induced dissociation

Introduction

Lipids comprise a diverse group of molecules that play important roles in membrane dynamics, storage of metabolic energy, and signaling [1, 2]. The complete assortment of molecular lipid species in a biological system is termed a lipidome and is governed by a network of metabolic pathways that synthesizes distinct lipid species by assembling or disassembling a multitude of hydrocarbon residues (e.g., fatty acids) and polar head groups (e.g., choline) [3]. Lipid species can be divided into several lipid categories and lipid classes based on their chemical structures [4]. The most abundant lipid categories in eukaryotic cells include glycerophospholipids, sphingolipids, glycerolipids, and sterol lipids. Dysfunctional regulation of lipid metabolism causes cellular lipotoxicity, impairs cellular processes, and contributes to the pathogenesis of disorders such as obesity, atherosclerosis, and neurodegeneration [5]. To improve the understanding of the regulation of lipidome composition during physiological and pathophysiological processes warrants lipidomics routines supporting quantitative monitoring of molecular lipid species on a global scale.

Correspondence to: Christer S. Ejsing; *e-mail:* cse@bmb.sdu.dk

Lipidomic techniques cover a broad range of mass spectrometry-based workflows affording extensive lipidome coverage with several hundreds of lipid species [3, 6–9]. These techniques are based on direct infusion MS (i.e., shotgun lipidomics) or liquid chromatography (LC)-MS [10–13]. A core component of all lipidomic platforms is the type of mass spectrometer employed, which spans sensitive low resolution triple quadrupole and ion trap instruments to high resolution hybrid quadrupole time-of-flight, ion trap-Orbitrap, and ion trap-Fourier transform ion cyclotron resonance (FT-ICR) machines offering high resolving power and high mass accuracy [14–17]. By shotgun lipidomics, lipid extracts are directly infused into the mass spectrometer, followed by identification and quantification of lipid species based on accurately determined masses and/or specific tandem mass analysis [10, 16]. Identified lipid species should be annotated by a shorthand nomenclature corresponding to the level of detail attainable by the mass analysis [18–20]. The detection of lipid species by high resolution FTMS analysis or by tandem mass analysis and detection of lipid class-specific fragment ions [e.g., m/z 184.0733 for phosphatidylcholine (PC) species] supports only annotation by "sum composition" (e.g., PC 34:1). In comparison, annotation by more detailed "molecular species composition" (e.g., PC 16:0-18:1) requires tandem mass analysis and detection of molecular structure-specific fragment ions [21]. Further in-depth structural analysis by ozone derivatization and structure-specific fragmentation analysis affords annotation by "defined molecular species composition," which can denote the double bond position within the fatty acid moieties of lipid species [e.g., PC 16:0-18:1(n-9)] [22] and the abundance of positional isomers [21, 23, 24].

The Orbitrap Fusion is a new generation of high resolution instrumentation made commercially available in 2013. This hybrid quadrupole-Orbitrap-ion trap mass spectrometer is equipped with three mass analyzers, two detectors, and two collision cells enabling complementary multi-stage fragmentation analysis using both quadrupole-based higher-energy collisional dissociation (HCD) and ion trap-based resonant-excitation collision-induced dissociation (CID). The ultra-high-field mass analyzer of the Orbitrap Fusion affords acquisition of FTMS spectra with resolving power up to 450,000 (full width at half maximum (FWHM) at m/z 200) at a transient duration of 1 s. The high resolving power at this scan speed is thus far unsurpassed by any other commercially available Orbitrap instrument, and at m/z 400 comparable to that of commonly used FT-ICR mass spectrometers operated with a transient duration of 1 s, as typically used for routine analysis [17, 25–27]. A key benefit of high resolving power for lipidomic analysis is the ability to accurately discriminate lipid species with isobaric nominal masses as well as their isotopes and, hence, support accurate lipid identification [17, 28]. Moreover, the capability of multi-stage fragmentation provides a new avenue for in-depth structural lipid analysis capable of exploiting differential fragmentation patterns obtained by CID and HCD ion activation and, as such, resolve isomeric lipid species [21]. Importantly, the Orbitrap Fusion offers a wide range of operational modes supporting in-depth lipidome analysis, but requires systematic

evaluation and optimization of instrument parameters in order to benchmark its performance and identify potential pitfalls.

Here, we report on the development and application of a novel shotgun lipidomics platform using the Orbitrap Fusion mass spectrometer equipped with an automated direct infusion nanoelectrospray ion source. To benchmark the platform for lipidomic analysis, we evaluated the ability to accurately distinguish isobaric lipid species and their isotopes, the isotopic fidelity (i.e., accuracy of relative isotopic abundances), the dynamic quantification range, and parameters for in-depth fragmentation analysis by HCD and CID. This systematic evaluation served as a guideline for developing a comprehensive acquisition method, termed MS^{ALL}, featuring high resolution FTMS analysis with a resolution setting of 450,000 for accurate lipid identification and quantification, and high resolution FTMS^2 analysis by sequential precursor ion fragmentation with combined HCD and CID and ITMS^3 analysis using dual CID for in-depth structural characterization of molecular glycerophospholipid species. The performance of the MS^{ALL} method for global lipidome analysis was evaluated by a comparative analysis of mouse cerebellum and hippocampus. This analysis demonstrated reproducible lipidome quantification of 311 lipid species encompassing 20 lipid classes, and the identification of 202 distinct molecular glycerophospholipid species by applying a novel high confidence filtering strategy requiring the detection of multiple molecular structure-specific fragment ions. The systematic evaluation of the performance characteristics of the Orbitrap Fusion-based platform presented herein validates its use for in-depth lipidome analysis.

Materials and Methods

Chemicals and Lipid Standards

Chemicals, solvents, and synthetic lipid standards were purchased from Sigma-Aldrich (St. Louis, MO, USA), Rathburn Chemicals (Walkerburn, Scotland), Avanti Polar Lipids (Alabaster, AL, USA), and Larodan Fine Chemicals (Malmö, Sweden).

Mouse Brain Tissue Sampling

Animal experiments were conducted in strict accordance with German law (in congruence with 86/609/EEC) for the use of laboratory animals and approved by the local animal welfare committee at the Johannes Gutenberg University Mainz. Male C57Bl/6 wild-type mice were euthanized by an overdose of ketamine via intraperitoneal injection. Subsequently, the mice were perfused intracardially with 4 °C 155 mM ammonium acetate, and the cerebellum and hippocampus were dissected. The tissues were frozen on dry ice and stored at –80 °C until further processing.

Lipid Extraction

Brain tissues were homogenized in 155 mM ammonium acetate and analyzed for total protein concentration using BCA

Protein Assay Kit (Thermo Scientific (Rockford, IL, USA)). Aliquots of tissue homogenates corresponding to 10 µg of total protein were subjected to lipid extraction by a modified Bligh and Dyer protocol executed at 4 °C [29]. Briefly, the tissue homogenates were spiked with internal lipid standard mix containing cholesteryl ester (CE) 19:0, triacylglycerol (TAG) 17:1/17:1/17:1, diacylglycerol (DAG) 19:0/19:0, lysophosphatidic acid (LPA) O-16:0, phosphatidic acid (PA) 17:0/14:1, lysophosphatidylserine (LPS) 17:1, phosphatidylserine (PS) 17:0/20:4, phosphatidylethanolamine (PE) O-20:0/O-20:0, lysophosphatidylcholine (LPC) O-17:0, PC O-18:1/O-18:1, phosphatidylinositol (PI) 17:0/20:4, phosphatidylglycerol (PG) 17:0/14:1, ceramide (Cer) 18:1;2/17:0;0, sphingomyelin (SM) 18:1;2/17:0;0, glucosylceramide (HexCer) 18:1;2/12:0;0, and sulfatide (SHexCer) 18:1;2/12:0;0. Next, the samples were added chloroform/methanol (2:1, v/v) and vigorously mixed for 1 h. Samples were subsequently centrifuged for 1 min at 500g to facilitate phase separation. The lower organic phase was subsequently transferred to a new tube and vacuum evaporated.

Mass Spectrometric Lipid Analysis

Lipid extracts and synthetic lipid standards were dissolved in chloroform/methanol (1:2, v/v) and subjected to mass spectrometric analysis using an Orbitrap Fusion Tribrid (Thermo Fisher Scientific, San Jose, CA, USA) equipped with a TriVersa NanoMate (Advion Biosciences, Ithaca, NY, USA). Aliquots of lipid extracts or synthetic lipid standards were loaded in 96-well plates, mixed with 13.3 mM and 1.3 mM ammonium acetate in 2-propanol for positive and negative ion mode analysis, respectively. Samples were infused using a back pressure of 1.25 psi and ionization voltage of ±0.95 kV [3]. All FTMS data were recorded using a max injection time of 100 ms, automated gain control at $2 \cdot 10^5$, two microscans, and a target resolution of 450,000 (FWHM at m/z 200), unless noted otherwise. All FTMS^2 data were acquired using max injection time of 100 ms, automated gain control at $5 \cdot 10^4$, one microscan, and a target resolution of 30,000, unless noted otherwise. All ITMS^3 data were acquired using max injection time of 200 ms, automated gain control at $1 \cdot 10^4$, and one microscan. All FTMS and ITMS data were acquired in profile mode, and using an ion transfer tube temperature of 80 °C and 125 °C for positive and negative ion mode, respectively. Positive ion mode MS^{ALL} analysis (see overview in Figure 4a) was performed using (1) high resolution FTMS analysis of the low m/z range 350–600 [monitoring LPC and lysophosphatidylethanolamine (LPE) species], (2) high resolution FTMS analysis of the high m/z range 500–1200 [monitoring SM, Cer, DAG, PC, ether-linked phosphatidylcholine (PC O-), PE, ether-linked phosphatidylethanolamine (PE O-) and TAG species], (3) sequential FTMS^2 analysis in 1.0008 u steps across the m/z range 400.3–1000.8 using a quadrupole ion isolation width of 1.0 u and HCD with normalized collision energy at 25%, (4) sequential FTMS^2 analysis in 1.0008 u steps across the m/z range 400.3–1000.8 using a quadrupole ion isolation width of 1.0 u and CID with collision energy at

33%, and (5) targeted ITMS^3 analysis for PE, monomethyl phosphatidylethanolamine (MMPE) and dimethyl phosphatidylethanolamine (DMPE) species using a quadrupole ion isolation width of 1.0 u and CID with normalized collision energy at 38% followed by ion trap ion isolation at width of 2.5 and CID with collision energy at 30%. Negative ion mode MS^{ALL} analysis was performed using (1) high resolution FTMS analysis of the low m/z range 370–660 [monitoring LPA, LPS, and lysophosphatidylinositol (LPI) species], (2) high resolution FTMS analysis of the high m/z range 550–1200 (monitoring PA, PS, PI, PG, and SHexCer species), (3) sequential FTMS^2 analysis in 1.0008 u steps across the m/z range 400.2–1000.7 using a quadrupole ion isolation width of 1.0 u and HCD with collision energy at 30%, (4) sequential FTMS^2 analysis in 1.0008 u steps across the m/z range 400.2–1000.7 using a quadrupole ion isolation width of 1.0 u and CID with collision energy at 33%, and (5) targeted ITMS^3 analysis for PC, PC, O- and PS species using a quadrupole ion isolation width of 1.0 u and CID with normalized collision energy at 38% followed by using ion trap ion isolation width of 2.5 and CID with collision energy at 30%. All FTMS^2 and ITMS^3 analyses were performed using data-independent acquisition (DIA) using precompiled target lists with precursor m/z values.

Annotation of Lipid Species

Lipid species were annotated as previously described [3, 6, 30]. For example, glycerophospholipid and glycerolipid species annotated by "sum composition" were denoted as: <lipid class><total number of C in fatty acid moieties>:<total number of double bonds in fatty acid moieties>(e.g., PI 34:1). Sphingolipid species annotated by "sum composition" were denoted as<lipid class><total number of C in the long-chain base and fatty acid moiety>:<total number of double bonds in the long-chain base and fatty acid moiety>;<total number of OH groups in the long-chain base and fatty acid moiety>(e.g., SM 35:1;2) [31]. Molecular glycerophospholipid species annotated by "molecular species composition" were denoted as: <lipid class><number of C in the first fatty acid moiety>:<number of double bonds in the second fatty acid moiety>–<number of C in the second fatty acid moiety>:<number of double bonds in the second fatty acid moiety>(e.g., PS 16:0-22:6).

Data Processing and Lipid Identification

Lipid species detected by MS^{ALL} using high resolution FTMS analysis were identified and quantified using ALEX software as previously described [32]. In short, lipid species detected by FTMS and annotated by sum composition were quantified by normalizing their intensity to the intensity of an internal lipid standard of identical lipid class and multiplying with the spike amount of the internal lipid standard and the type I isotope correction factor [32–34]. Molecular glycerophospholipid species detected by MS^{ALL} using FTMS^2 and ITMS^3 were identified using a prototype ALEX^{123} software combined with a

prototype lipid fragmentation database. Fragment ion information was compiled by systematic fragmentation analysis of (only) synthetic glycerophospholipid standards in both positive and negative ion mode. This analysis demonstrated that glycerophospholipid species release multiple fragment ions corresponding to both direct release of fatty acid moieties (e.g., acyl anions in negative ion mode) and neutral loss of fatty acid moieties (e.g., as ketenes in both positive and negative ion mode). Using this information, we constructed a library of more than 4500 molecular glycerophospholipid species having fatty acid moieties with 10 to 26 carbon atoms and containing 0 to 6 double bonds. For all molecular glycerophospholipid species, we computed m/z values of expected fragment ions based on the fragmentation patterns observed for the synthetic glycerophospholipid standards. This fragmentation database was used by the prototype ALEX[123] software for identifying fragment ions detected by FTMS[2] and ITMS[3] analysis using m/z tolerance settings of ±0.005 u and ±0.1 u, respectively. The ALEX[123] output format was saved in relational database format [32] and further processed for data visualization, filtering, and molecular glycerophospholipid species identification using Tableau Desktop (Tableau Software). An intensity filter was applied for identification requiring that ions detected by FTMS, FTMS[2] and ITMS[3] should have intensity higher than 2000, 500 and 1 count, respectively (values determined by manual assessment of spectral quality), and be detected in at least half of all sample injections. The numbers of molecular glycerophospholipid species identified by both positive and negative FTMS[2] analysis using HCD, FTMS[2] analysis using CID and ITMS[3] analysis were compared using Venn Diagram Online (www.bioinformatics.lu/venn.php).

Results and Discussion

A Shotgun Lipidomics Platform Featuring an Orbitrap Fusion Mass Spectrometer

A new shotgun lipidomics platform was established by combining an Orbitrap Fusion mass spectrometer with a TriVersa Nanomate nanoelectrospray ion source. This platform allows harnessing the unprecedented analytical capabilities of the Orbitrap Fusion in conjunction with automated direct infusion nanoelectrospray ionization supporting sensitive lipidome analysis at a high throughput. The unique hardware configuration of the Orbitrap Fusion mass spectrometer defines three instrumental factors that in combination specify multiple modes of instrument operation (Table 1). These instrumental factors include (1) quadrupole-based ion isolation or ion trap-based ion isolation, (2) ion activation by either quadrupole-based HCD or ion trap-based resonant-excitation CID, and (3) ion detection using either the high resolution Orbitrap analyzer (six available resolution settings for FTMS analysis) or the low resolution ion trap analyzer (ITMS analysis). For survey MS analysis, one out of seven available modes of ion detection can be selected (Table 1). Performing MS[2] analysis requires

specification of the mode of ion isolation (two available modes), ion activation (two available modes), and ion detection (seven available modes), which collectively provide 28 different possible modes of operation. For MS[n≥3] analysis only the settings for ion activation and ion detection need to be defined as fragment ions are isolated in the ion trap prior to the subsequent fragmentation analysis. Notably, the Orbitrap Fusion also supports various data acquisition procedures including data-dependent acquisition (DDA) and data-independent acquisition (DIA) of MS and MS[n] spectra triggered by a variety of parameters, including intensity threshold, exclusion lists, and inclusion lists (Table 1). This repertoire of operational modes and data acquisition procedures provides a wide range of analytical capabilities that can be deployed for in-depth lipidome analysis. However, instrumental settings and parameters warrant systematic evaluation in order to optimize instrument performance for lipidome analysis and to identify potential limitation and pitfalls.

Evaluation of High Resolution FTMS Analysis and Isotope Fidelity

High resolution FTMS analysis supports accurate identification of lipid species with mass accuracy at the low parts-per million (ppm) range and, depending on mass resolution, baseline separation of a wide assortment of lipid species with isobaric nominal masses [16]. These analytical hallmarks support absolute quantification of lipid species annotated by sum composition without recourse to tandem mass analysis as required on triple quadrupole machines [6, 16, 30]. However, FTMS spectral data quality can be compromised by deviating isotopic fidelity (i.e., accuracy of relative isotopic abundances), shifting of accurate masses, and peak coalescence due to space charging effects [35, 36], which can bias lipid identification and quantification. In addition, mass resolution of FTMS analysis decays exponentially as function of m/z [25], which can also complicate lipid identification and bias quantification depending on the m/z of monitored lipid species. Notably, the Orbitrap Fusion is equipped with a new ultra-high-field Orbitrap mass analyzer and utilizes a dedicated apodization algorithm (eFT) that allows acquisition of FTMS spectra with a mass resolution up to 450,000 (FWHM at m/z 200) [25, 37, 38]. To evaluate the efficacy of the higher resolving power of FTMS analysis on the Orbitrap Fusion, we analyzed a sample containing three pairs of synthetic lipid species differing by one double bond [i.e., Cer 42:1;2 and Cer 42:2;2, PC 34:1 and PC 34:2, TAG 54:1 and TAG 54:2 (Figure 1)]. Each pair was mixed at a molar ratio such that the intensity of the mono-isotopic species with one double bond [e.g., PC 34:1(M0), m/z 760.5851] yielded an intensity comparable to the intensity of the second isotope of the species with two double bonds [e.g. PC 34:2(M2), m/z 760.5758]. To benchmark the resolving power of FTMS on the Orbitrap Fusion, we also analyzed the sample using an LTQ Orbitrap XL (Figure 1). Both instruments were operated at their highest mass resolution setting. The analysis demonstrated that FTMS on the Orbitrap Fusion can effectively distinguish the

Table 1. Operational Modes and Data Acquisition Procedures Supported by the Orbitrap Fusion Mass Spectrometer

	Instrumental factors			Data acquisition procedures
	Ion isolation	Ion activation	Ion detection	
MS analysis			ITMS R1000	DDA of SIM[a]
			FTMS R15000	based on MS data
			FTMS R30000	DIA of SIM
			FTMS R60000	based on target list
			FTMS R120000	
			FTMS R240000	
			FTMS R450000	
MS[2] analysis	Quadrupole	HCD in the quadrupole	ITMS R1000	DDA of MS[2] based on MS data
	Ion trap	CID in the ion trap	FTMS R15000	DIA of MS[2] based on target list
			FTMS R30000	
			FTMS R60000	
			FTMS R120000	
			FTMS R240000	
			FTMS R450000	
MS[n≥3] analysis	Ion trap	HCD in the quadrupole	ITMS R1000	DDA of MS[n]
		CID in the ion trap	FTMS R15000	based on MS[n-1] data
			FTMS R30000	DIA of MS[n]
			FTMS R60000	based on target list
			FTMS R120000	
			FTMS R240000	
			FTMS R450000	

[a] SIM: selected ion monitoring
[b] Currently not supported if MS[n-1] data is acquired using DIA

mono-isotopic peak and the second isotope peak of lipid species having one or two double bonds, respectively (Figure 1a, c, e). For example, the mono-isotopic peak of PC 34:1(M0) could be resolved from the second isotope of PC 34:2(M2) (Figure 1c). Importantly, this result demonstrates that the higher resolving power of the Orbitrap Fusion allows distinguishing isotopes of individual lipid species with m/z up to 900, which spans the m/z range for majority of lipid species in bacteria, yeast, and mammals. In comparison, FTMS analysis by the LTQ Orbitrap XL could only partially distinguish the mono-isotope of Cer 42:1;2(M0) from the second isotope of Cer 42:2;2(M2) (Figure 1b), and failed to separate the pairs of PC and TAG species having higher m/z values (Figure 1d, f).

To assess the accuracy of the isotope pattern measured by FTMS analysis (i.e., isotopic fidelity), we next overlaid recorded spectra with simulated isotope profiles (Figure 1). This analysis showed that FTMS data recorded on both the Orbitrap Fusion and the LTQ Orbitrap XL closely matched the simulated isotopic profile of the mono-isotopic peak (M0) and first isotope peak (M1) of Cer 42:2;2, PC 34:2, and TAG 54:2. More pronounced deviations were observed between simulated and measured isotopic profiles for ion clusters containing the second isotope (M2) of Cer 42:2;2, PC 34:2, and TAG 54:2 and the corresponding mono-isotopic (M0) peak of Cer 42:1;2, PC 34:1, and TAG 54:1, respectively. In all instances, we observed that the measured FTMS profiles were underestimated compared with the simulated isotope profiles. Similarly, comparing the spectral profiles of isotope clusters containing the third isotope (M3) of Cer 42:2;2, PC 34:2, and TAG 54:2 and the corresponding first isotope (M1) of Cer 42:1;2, PC 34:1, and TAG 54:1, respectively, we again noticed a systematic

underestimation of the measured profiles compared with simulated isotope profiles. Importantly, in all instances, the FTMS data recorded on the Orbitrap Fusion better matched the simulated isotope profiles compared with that of FTMS data obtained using the LTQ Orbitrap XL.

To more systematically evaluate the isotopic fidelity of FTMS analysis on the Orbitrap Fusion and the LTQ Orbitrap XL, we next analyzed a set of samples where the molar ratio between synthetic TAG 54:2 and TAG 54:1 was systematically titrated. For example, we analyzed samples containing only TAG 54:2 or TAG 54:1, or various mixtures including TAG 54:2/TAG 54:1 (5:1, mol/mol), TAG 54:2/TAG 54:1 (1:1, mol/mol), and TAG 54:2/TAG 54:1 (1:5, mol/mol). As a proxy for isotopic fidelity, we determined the isotopic defects for each TAG isotopologue by computing the difference between the measured relative intensity and the simulated relative intensity of a given TAG isotopologue. To assess isotopic fidelity, we plotted the isotope defect as a function of the molar fraction of TAG 54:1 (Figure S1 in Supporting Information). This analysis showed that the isotopic defects by FTMS analysis on the Orbitrap Fusion were within an interval of –9% [for TAG 54:2(M2)] to 4% [for TAG 54:2(M0)] (Figure S1a). Notably, the isotopic defects for mono-isotopic TAG 54:2 and TAG 54:1, which are the ions used for identification and quantification, were minor and ranged between 0% and 4% and –5% and 0%, respectively. In comparison, the isotopic defects observed by FTMS analysis on the LTQ Orbitrap XL were within the interval of –18% to 3% [for TAG 54:2(M2)] (Figure S1b). Based on these results, we conclude that the isotopic fidelity of FTMS analysis using a resolution setting of 450,000
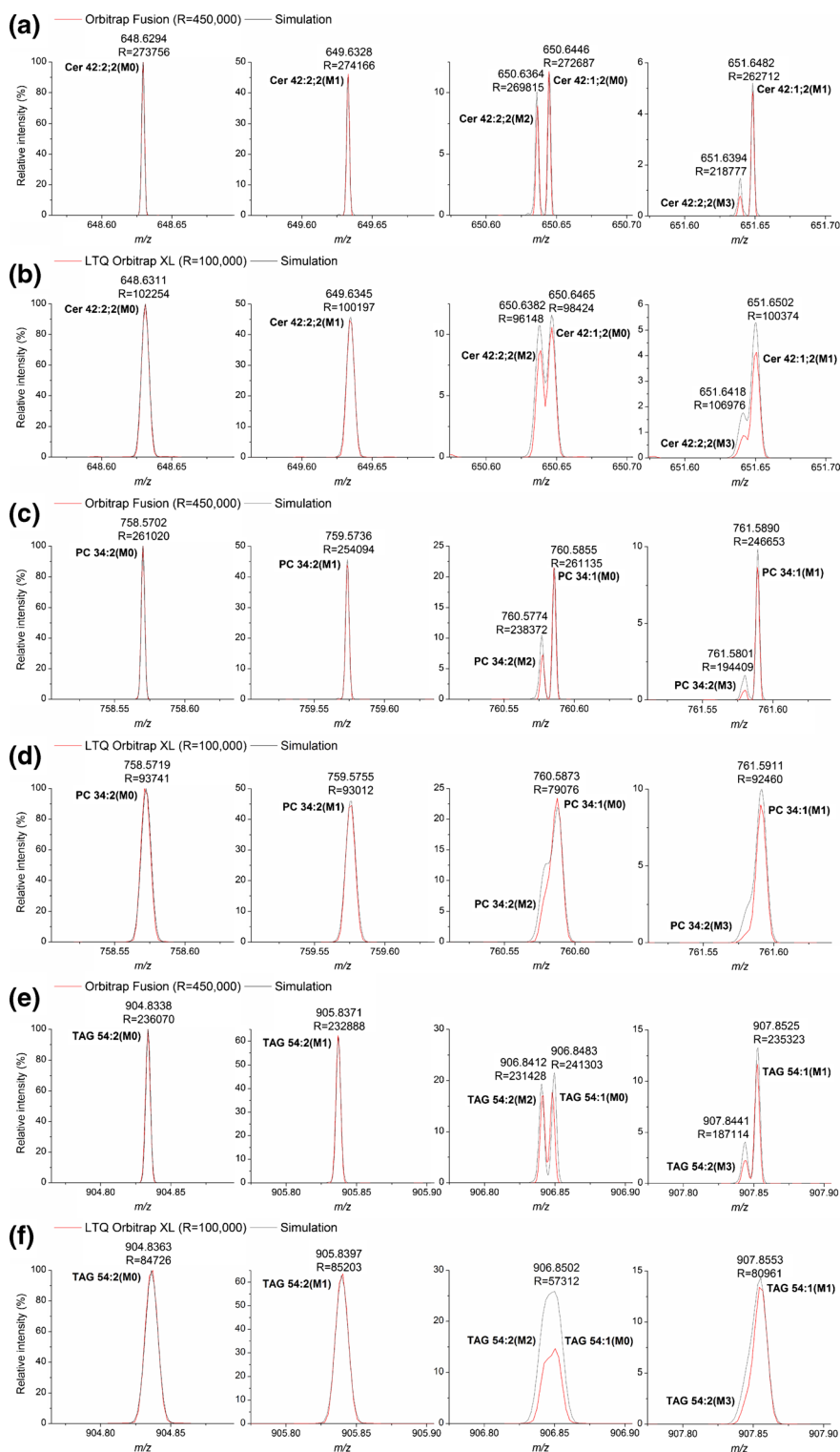
Figure 1. Comparison of measured and simulated isotope profiles of mixtures of synthetic Cer, PC, and TAG lipids having a difference of one double bond. Spectral data was obtained using the Orbitrap Fusion operated with a resolution setting of 450,000 and the LTQ Orbitrap XL operated with a resolution setting of 100,000. (**a**) Orbitrap Fusion: FTMS analysis of Cer 42:2;2 and Cer 42:1;2 at a molar ratio of 9:1. (**b**) LTQ Orbitrap XL: FTMS analysis of Cer 42:2;2 and Cer 42:1;2 at a molar ratio of 9:1. (**c**) Orbitrap Fusion: FTMS analysis of PC 34:2 and PC 34:1 at a molar ratio of 5:1. (**d**) LTQ Orbitrap XL: FTMS analysis of PC 34:2 and PC 34:1 at a molar ratio of 5:1. (**e**) Orbitrap Fusion: FTMS analysis of TAG 54:2 and TAG 54:1 at a molar ratio of 5:1. (**f**) LTQ Orbitrap XL: FTMS analysis of TAG 54:2 and TAG 54:1 at a molar ratio of 5:1. Spectra recorded on the LTQ Orbitrap XL feature a minor but systematic calibration m/z offset of +3.5 ppm. Simulations of isotope patterns (black line) were performed using QualBrowser software and applied the calibration m/z offset to assist the visual comparison between spectral and simulated profiles

on the Orbitrap Fusion is acceptable and adequate for supporting accurate lipid identification and quantification.

Evaluation of Dynamic Quantification Range

Absolute quantification of lipids is a key tenet of high resolution shotgun lipidomics platforms. To evaluate the dynamic quantification range of FTMS analysis on the Orbitrap Fusion, we analyzed a dilution series of two synthetic SM standards where one species, SM 35:1;2 (molecular species SM 18:1;2/17:0;0), was titrated across a concentration range of 0.8 nM to 6 μM and the other species, SM 30:1;2 (molecular species SM 18:1;2/12:0;0), was kept constant. To evaluate the dynamic quantification range, we plotted the intensity ratio between the two SM species as a function of their molar ratio (Figure 2a). This assessment demonstrated that the FTMS response was linear with a slope value of approximately one across four orders of magnitude. The limit of quantification of the FTMS analysis was approximately 2 nM SM 35:1;2 (corresponding to the molar ratio value of 0.02 in Figure 2a).

A similar evaluation was performed using the neutral lipid standards TAG 51:3 (molecular species TAG 17:1-17:1-17:1) and deuterated TAG 51:1 (molecular species TAG 17:0-17:1-17:0+D5) (Figure 2b). This experiment showed that also the TAG quantification range was linear with a slope value of approximately one across four orders of magnitude and featured a limit of quantification of approximately 1 nM TAG 51:3 (corresponding to molar ratio value of 0.005 in Figure 2b). Notably, the dynamic quantification range and limit of quantification of FTMS analysis on the Orbitrap Fusion are similar to shotgun lipidomic analysis on other FTMS instruments [3], hybrid quadrupole time-of-flight and triple quadrupole instruments [39]. Based on these results, we conclude that FTMS

analysis on the Orbitrap Fusion is applicable for quantitative lipidome analysis.

Evaluation of HCD and CID for Structural Lipid Characterization

Fragmentation of molecular lipid species produces a combination of lipid class-specific fragment ions and molecular structure-specific fragment ions [21, 40–46]. For example, in negative ion mode, all PI lipids release the lipid class-specific fragment ion with m/z 241.0119 and also molecular structure-specific fragments including acyl anions and those deriving from neutral loss of fatty acid moieties as ketenes (Figure 3a, b). Such fragmentation patterns can be used for (1) confirming the identity of lipid species detected by high resolution FTMS analysis and annotation of lipid species by "sum composition" (e.g., PI 38:4), (2) identifying the molecular composition of apolar hydrocarbon chains including fatty acid, plasmanyl, plasmenyl, and long-chain base moieties and annotation of lipid species by molecular species composition (e.g., PI 18:0-20:4), and (3) for quantification of isomeric lipid species (e.g., PI 18:1-20:3 versus PI 16:0-22:4). Notably, the Orbitrap Fusion affords fragmentation analysis using both HCD and CID. These ion activation mechanisms produce different stoichiometries of fragment ions (Figure 3a, b), which in combination can be used for recording complementary fragment ion datasets. Moreover, the Orbitrap Fusion allows acquisition of high resolution FTMS^2 spectra, which affords detection of especially low abundant structure-specific fragment ions with high mass accuracy and, as such, should facilitate higher confidence identification of molecular lipid species compared with fragmentation analysis using low resolution machines such as triple quadrupole instruments. Notably, the
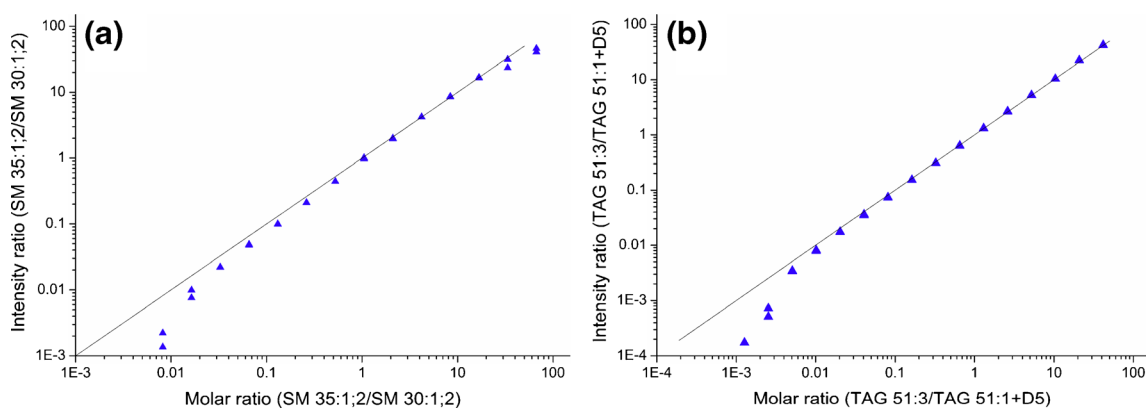

Figure 2. Dynamic quantification range of FTMS analysis on the Orbitrap Fusion. (**a**) Synthetic SM 35:1;2 was titrated (0.8 nM to 6 μM) relative to a constant amount of synthetic SM 30:1;2 (127 nM). Lipid mixtures were analyzed in positive ion mode by FTMS using a target resolution of 240,000. The *x*-axis shows the concentration of SM 35:1;2 relative to the concentration of SM 30:1;2 (i.e., molar ratio). The *y*-axis shows the intensity of protonated SM 35:1;2 relative to the intensity of protonated SM 30:1;2. The line indicates the linear function with slope 1. Data points represent two replicate analyses per sample. (**b**) Synthetic TAG 51:3 was titrated (0.3 nM to 9.5 μM) relative to a constant amount of synthetic and deuterated TAG 51:1+D5 (227 nM). The TAG mixture was analyzed as in panel (**a**). The *x*-axis shows the molar ratio of TAG 51:3 relative TAG 51:1+D5. The *y*-axis shows the intensity of ammoniated TAG 51:3 relative to the intensity of ammoniated TAG 51:1+D5. Data points represent two replicate analyses per sample
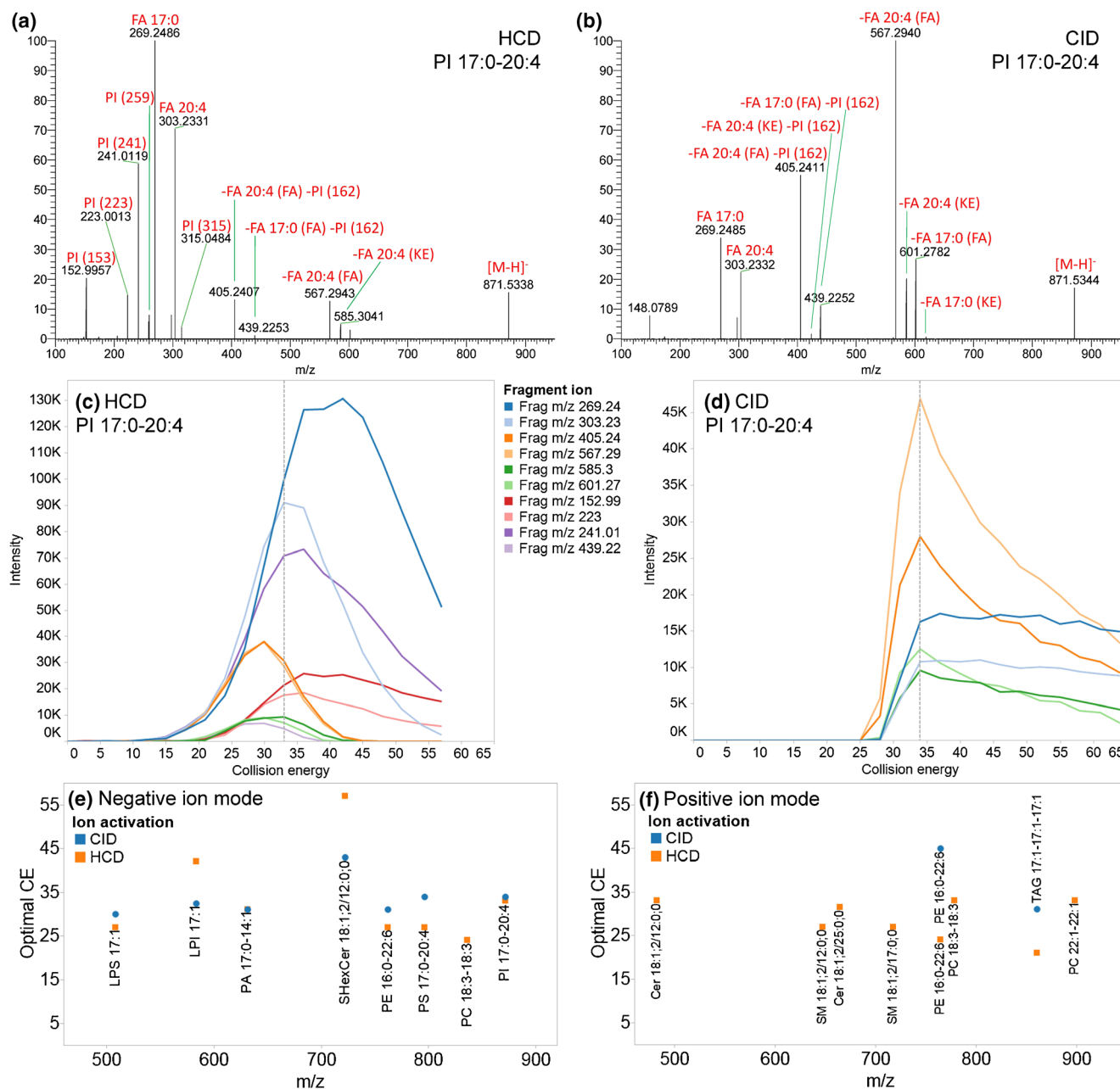
Figure 3. Evaluation of HCD and CID ion activation for structural lipid analysis. (**a**) Negative ion mode HCD-FTMS^2 spectrum of synthetic PI 17:0-20:4. The normalized collision energy and target mass resolution were 36% and 15,000, respectively. The spectrum is annotated to highlight lipid class-specific fragments (e.g., PI 153 and PI 241) and molecular structure-specific fragments [e.g., FA 17:0, '–FA 20:4 (KE)' (neutral loss of FA 20:4 as a ketene) and '–FA 17:0 (FA) –PI 162' (neutral loss of FA 17:0 as a fatty acid (FA) and neutral loss of inositol)]. (**b**) Negative ion mode CID-FTMS^2 spectrum of PI 17:0-20:4. The normalized collision energy and target mass resolution were 34% and 15,000, respectively. The spectrum is annotated as in panel (**a**). (**c**) Negative ion mode HCD-FTMS^2 analysis of PI 17:0-20:4. Plot shows fragment ion intensity as a function of collision energy. The vertical line displays the optimal collision energy, 33%, for detection of all fragment ions. (**d**) Negative ion mode CID-FTMS^2 analysis of PI 17:0-20:4. Plot shows fragment ion intensity as a function of collision energy. The vertical line displays the optimal collision energy, 34%, for detection of all fragment ions. Note that the legend 'Fragment ion' displays color coding for both panel (**c**) and panel (**d**). (**e**) Plot of optimal collision energy as a function of precursor *m/z* for negative ion mode analysis. (**f**) Plot of optimal collision energy as a function of precursor *m/z* for positive ion mode analysis

Orbitrap Fusion is also capable of further in-depth structural characterization by multi-stage activation (MS^n) using combinations of HCD and CID (Table 1). To build an analytical routine using combinatorial fragmentation analysis with HCD and CID requires evaluation and optimization of multiple parameters, including specification of optimal collision energies

for detection of fragment ions from different lipid classes. The Orbitrap Fusion, as well as all other Orbitrap instrumentation, uses a 'normalized collision energy,' which in principle should equalize for differences in m/z between lipid analytes and ideally different ion activation mechanisms. In order to evaluate and optimize normalized collision energy settings for structural analysis of lipid species, we carried out a series of FTMS^2 experiments using different collision energies and ion activation by HCD and CID (Figure 3c, d). Using this information, we determined the optimal collision energy required for fragmentation analysis of a range of lipid species relevant for biological systems (Figure 3e, f). Our analysis revealed that one optimal value for normalized collision energy is not applicable for all lipid species and also not identical for ion activation by HCD and CID. For example, optimal collision energy for detection of sulfatide (SHexCer 18:1;2/12:0;0)-derived fragment ions in negative ion mode were 57% and 43% when using HCD and CID, respectively. In positive ion mode, the optimal collision energy for detection of PE 16:0-22:6-derived fragment ions were 24% and 45% when using HCD and CID, respectively. Importantly, a difference of only ±5% in collision energy can significantly reduce the optimal detection of fragment ions, especially when using CID (Figure 3d). Notably, the optimal collision energies for detection of fragment ions from some lipid species (e.g., PI 17:0-20:4, PA 17:0-14:1) were similar for both HCD and CID (Figure 3e). Based on these results, we conclude that optimal collision energies for detection of fragment ions is lipid class-dependent and should be determined and applied in order to optimize the performance of lipid structural analysis. Moreover, we conclude that FTMS^2 analysis using both HCD and CID allows acquisition of complementary fragmentation patterns of molecular lipid species, and that low abundant structure-specific fragment ions, such as neutral loss of fatty acid moieties, can be detected with high mass accuracy. In addition, evaluation of MS^3 fragmentation analysis showed that it can be used for identifying molecular structure-specific fragment ions released from several classes of glycerophospholipids (data not shown) [21].

Evaluation of Ion Isolation Efficiency for Fragmentation Analysis

Ion isolation is a critical determinant of the sensitivity and specificity of fragmentation analysis. Especially the ion isolation width is of importance since it is key for limiting false-positive identification of lipid species caused by potential interference from co-isolation and fragmentation. Reducing the ion isolation width to approximately 1 u, as required for the specificity of shotgun lipidomic analysis, causes a loss of precursor ion intensity and consequently affects the sensitivity of fragmentation analysis. The Orbitrap Fusion affords both quadrupole-based and ion trap-based ion isolation, each with a distinct set of analytical advantages. Quadrupole ion isolation is fast and occurs at the front-end of the instrument, whereas ion trap isolation occurs at the distal region of the instrument and offers, in principle, more efficient trapping of ions but is prone to promote fragmentation and loss of labile lipid ions such as Cer and PC species with formate adducts [47]. To evaluate the performance of quadrupole-based and ion trap-based ion isolation, we performed two experiments. The first experiment was designed to evaluate the impact of quadrupole ion isolation width on the intensity of isolated precursor ion and co-isolation of neighboring ions. To this end, we performed FTMS^2 analysis of m/z 778.5, corresponding to mono-isotopic precursor ion of synthetic PC 36:6 (molecular species PC 18:3-18:3), using different quadrupole ion isolation widths and monitored the intensities of the mono-isotopic precursor ion and its first and second isotope (Figure S2a in Supporting Information). This analysis demonstrated that using a quadrupole ion isolation width of 1.0 u yielded a 33% loss of mono-isotopic precursor ion intensity compared with using a quadrupole ion isolation width of 16 u, and a limited co-isolation of the first isotope (0.8% relative to the intensity of the mono-isotopic ion) and no co-isolation of the second isotope (Figure S2b). Notably, using an ion isolation width of 2.0 u yielded a 22% loss of the mono-isotopic precursor ion, but caused a pronounced co-isolation of the first isotope of PC 18:3-18:3 (M1, 24% relative to the intensity of the mono-isotopic ion). Based on this analysis, we conclude that MS^2 analysis with high analytical specificity (i.e., limited co-isolation of precursor ions with a nominal mass difference of 1 u) should be performed using a quadrupole ion isolation width of 1.0 u or lower.

In the second experiment, we compared the ion isolation profile of quadrupole-based and ion trap-based ion isolation. To this end, we performed MS^2 analyses of synthetic TAG 51:3 (molecular species TAG 17:1-17:1-17:1) using both quadrupole and ion trap ion isolation. We systematically ramped the precursor m/z value used for ion isolation and monitored the intensities of mono-isotopic TAG 51:3 and its first and second isotope (Figure S2c, d in Supporting Information). We observed that using an ion trap isolation width of 1.9 u yielded an effective ion isolation width of approximately 1 u (and not ~2 u as expected), corresponding to that observed when using a quadrupole ion isolation width of 1.0 u (Figure S2c, d). Moreover, we also observed that performing both quadrupole and ion trap ion isolation at m/z 860.8 yielded no significant co-isolation of the first isotope of TAG 51:3 (M1), thus allowing specific lipid precursor ion isolation for structural analysis. We note that similar results were obtained analyzing a synthetic PC standard (data not shown). Based on these results, we conclude that MS^2 analysis using both quadrupole and ion trap ion isolation allows effective and specific isolation of lipid precursor ions. In addition, we recommend careful evaluation and optimization of especially ion trap ion isolation parameters when used for structural characterization of lipid species.

Shotgun Lipidomics by MS^{ALL}

Having evaluated the performance and operational characteristics of the Orbitrap Fusion, we next developed a shotgun lipidomic routine for in-depth lipidome analysis utilizing a

wide range of operational modes supported by the machine. To this end, we devised a novel acquisition method that we term MS^{ALL}, which combines high mass resolution FTMS analysis for lipid quantification, and MS^2 and MS^3 analysis for structural characterization of molecular lipid species. We note that this method can be extended to include additional dimensions of multistage activation (e.g., MS^4). The design of the MS^{ALL} method includes (1) survey FTMS analysis using a resolution setting of 450,000, (2) $FTMS^2$ analysis using HCD, (3) $FTMS^2$ analysis using CID, and (4) $ITMS^3$ analysis using CID-CID ion activation (Figure 4). The survey FTMS analysis was designed to include two FTMS scans covering a low m/z range and high m/z range in order to maximize the sensitivity of the Orbitrap mass analysis [48]. We note that the boundaries of the scan ranges were chosen to cover specific lipid classes and respective internal standards. For example, the scan range+FTMS m/z 350–600 was used for monitoring LPC and LPE species, whereas+FTMS m/z 550–1201 was used for monitoring Cer, SM, HexCer, PC, PC O-, PE, PE O-, DAG, and TAG species. The $FTMS^2$ fragmentation was performed using quadrupole-based ion isolation with a width of 1.0 u (see above), a resolution setting of 30,000, and DIA using target lists having 601 precursor ion m/z values that guide sequential recording of $FTMS^2$ data across the mass range of m/z 400 to 1000 in increments of 1.0008 Da. We note that this mode of operation is similar to MS/MS^{ALL} on hybrid quadrupole time-of-flight instruments [15]. However, the MS/MS^{ALL} approach does not support MS^n analysis using combined HCD and CID ion activation and only makes use of MS/MS data for identification and quantification. The $ITMS^3$ fragmentation was performed using quadrupole-based ion isolation with a width 1.0 u followed by ion trap-based ion isolation with a width 2.5 u. For $ITMS^3$ analysis, we also made use of DIA to perform in-depth characterization of glycerophospholipid species that release lipid class-specific fragment ions during MS^2 fragmentation (e.g., neutral loss of 141 by PE species in positive ion mode) (Figure 4a, e). We note that the current design of the MS^3 analysis can be extended for in-depth structural characterization of, for example, sphingolipid and TAG species. In order to benchmark the MS^{ALL} method, we performed a comparative lipidome analysis of mouse cerebellum and hippocampus. The experimental design included four biological replicates of each tissue, which were subjected to lipid extraction using internal lipid standards and analyzed by MS^{ALL} in positive and negative ion mode using two replicate injections per sample. In total we acquired 32 data files, which were processed for lipidome quantification using the FTMS data and for identification of distinct molecular glycerophospholipid species using the $FTMS^2$ and $ITMS^3$ data.

Quantitative Lipidome Analysis

For quantitative lipidome analysis, we processed the high resolution FTMS data using ALEX software [32]. ALEX software affords identification of lipid species detected by high resolution FTMS analysis and compiles output data in a database table format. This allows tracking all experimental data (e.g., originating .RAW file name, lipid species intensity, measured m/z), and implementing workflows for data normalization and visualization using database exploration tools such as open source Orange [49] and Tableau Desktop, respectively. Using ALEX software, we identified and calculated the molar abundances of 311 lipid species encompassing 20 lipid classes. These lipid species were annotated by sum composition and detected in at least half of all sample injections. Notably, 183 of the quantified lipids were glycerophospholipid species with two hydrocarbon moieties attached either via ester-linkages (diacyl species) or an ester- and an ether-linkage (plasmanyl or plasmenyl species). In comparison, a recent characterization of mouse forebrain by LC and triple quadrupole mass spectrometry quantified 325 lipid species annotated by sum composition, out of which 161 were glycerophospholipid species [50]. This result demonstrates the efficacy of the Orbitrap Fusion-based platform for extensive identification of lipid species by high resolution FTMS analysis.

Evaluating the molar abundances of lipid classes in cerebellum and hippocampus across all sample injections showed only minor differences between the tissues; hippocampus displays a slightly higher level of PE and lower level of PE O- compared with cerebellum (Figure 5a). Comparing the composition of lipid species, however, showed more pronounced differences; for example, the species PC 32:0, PC 36:4, and PC 38:4 were enriched in hippocampus compared with cerebellum, and the species PC 38:6 and PC 40:6 were enriched in cerebellum compared with hippocampus (Figure 5b). Notably, the obtained composition of lipid classes and lipid species in cerebellum and hippocampus is consistent with previous reports on mouse brain lipid composition [32, 50]. Based on these results, we conclude that the MS^{ALL} routine with FTMS analysis using a resolution setting of 450,000 affords reproducible and comprehensive lipidome quantification.

Identification of Molecular Glycerophospholipid Species by MS^2 and MS^3 Analysis

Having benchmarked the MS^{ALL} method for quantitative lipidomics, we next evaluated its efficacy for identification of molecular lipid species. While evaluating fragmentation analysis, we noted that $FTMS^2$ afforded detection of several low abundant structure-specific fragment ions with high mass accuracy (Figure 3a, b and Figure 4c, d). For example, by negative ion mode $FTMS^2$ analysis of synthetic PI 17:0-20:4, we detected 10 structure-specific fragment ions providing information about the fatty acid moiety composition and another 5 PI class-specific fragment ions (Figure 3a, b). $FTMS^2$ analysis of the same PI species in positive ion mode allowed detection of four structure-specific fragment ions and one PI class-specific fragment ion (data not shown). Systematic positive and negative ion mode $FTMS^2$ analysis of other (asymmetric) glycerophospholipid species, including PC, PC O-, PE, PE O-, PA, PS, PG, MMPE, and DMPE species, demonstrated detection of at least four structure-specific fragment ions in any ion
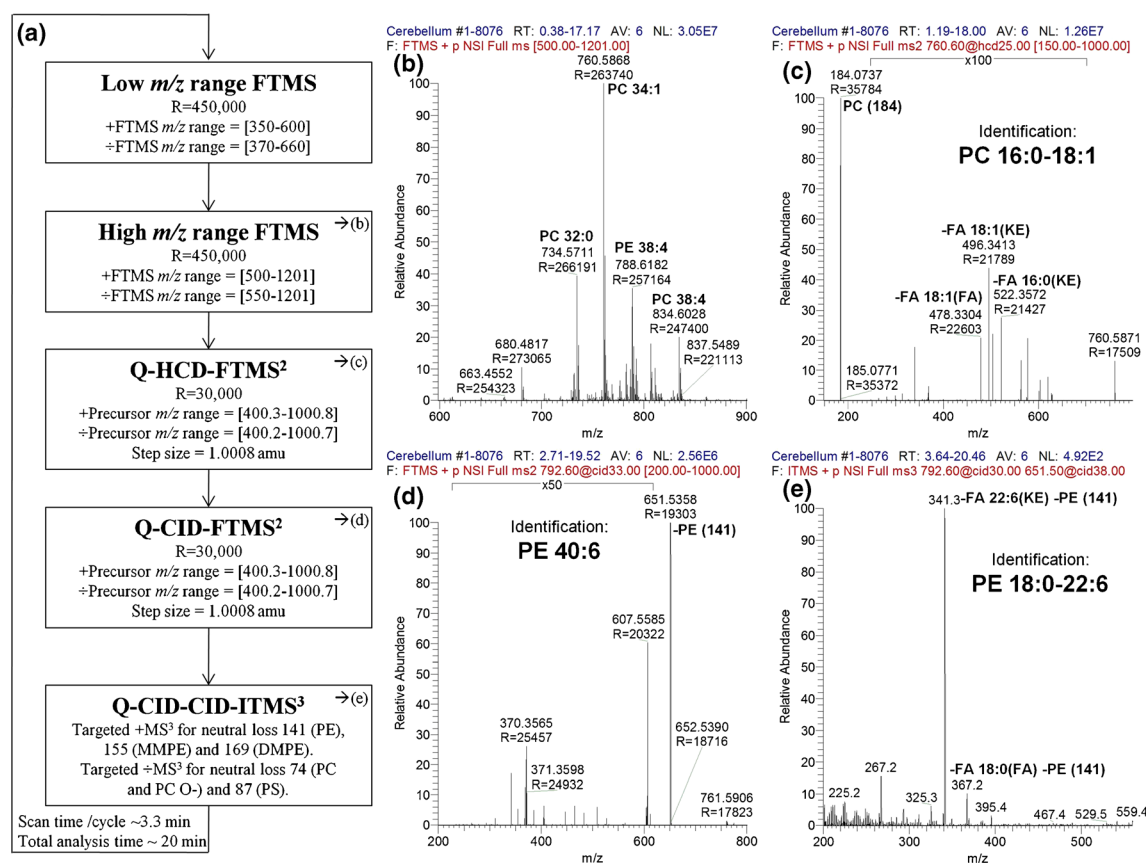
Figure 4. Overview of the MS[ALL] method and examples of acquired MS[n] spectra. (**a**) The MS[ALL] method includes five multiplexed MS analyses: (1) high mass resolution FTMS analysis in the low *m/z* range, (2) high resolution FTMS analysis in the high *m/z* range, (3) sequential FTMS[2] analysis using quadrupole ion isolation and HCD, (4) sequential FTMS[2] analysis using quadrupole ion isolation and CID, and (5) targeted ITMS[3] analysis for glycerophospholipid species using quadrupole ion isolation and CID followed by ion trap-based ion isolation and CID. An MS[ALL] method was designed for both positive and negative ion mode. (**b**) High resolution FTMS spectrum of a mouse cerebellum lipid extract. Identified lipid species are annotated by sum composition. (**c**) FTMS[2] spectrum of *m/z* 760.6 acquired using HCD. The identified lipid species PC 16:0-18:1 is annotated by molecular species composition based on the neutral loss of fatty acid moieties as indicated in the figure. (**d**) FTMS[2] spectrum of *m/z* 792.6 acquired using CID. The identified lipid species PE 40:6 is annotated by sum composition based on neutral loss of 141.019. (**e**) ITMS[3] spectrum of *m/z* 792.6*m/z* 651.5 using CID-CID. The identified lipid species PE 18:0-22:6 is annotated by molecular species composition based on the neutral loss of fatty acid moieties as indicated in the figure

mode. For example, FTMS[2] fragmentation of PC 16:0-18:1 in positive ion mode allowed detection of four low abundant structure-specific fragment ions corresponding to the neutral loss of the fatty acid moieties (Figure 4c). Based on these observations, we rationalized that low abundant fragment ions detected with high mass resolution and mass accuracy can be utilized for higher confidence identification of molecular lipid species compared with only using a limited set of intense fragment ions such as acyl anion [34]. Notably, low abundant fragment ions are typically not used for lipid identification in large-scale lipidomic analyses. Moreover, no software solutions and no lipid fragmentation databases are currently available for supporting identification of molecular lipid species using combinations of low abundant and intense structure-specific fragment ions detected using both HCD and CID. Hence, in order to enable identification of molecular lipid species detected by the MS[ALL] approach, we compiled a prototype lipid fragmentation database and a

prototype software tool for processing MS[ALL] fragmentation data. The prototype lipid fragmentation database contains more than 4500 molecular glycerophospholipid species with *m/z* values for structure-specific fragment ions and lipid class-specific fragment ions predicted based on fragmentation analysis of representative standards. Presently, the prototype database only contains glycerophospholipids with two hydrocarbon moieties, either as two fatty acid moieties or as an ether moiety and a fatty acid moiety. For PE, MMPE, DMPE, PC, PC O-, and PS species, we also added MS[3] fragmentation information on structure-specific fragments. The developed prototype software, termed ALEX[123], queries MS[2] and MS[3] data using information in the lipid database for identification of molecular lipid species using structure-specific and lipid class-specific fragment ions. Notably, the ALEX[123] software was designed to support independent processing of FTMS[2], ITMS[2], FTMS[3], and ITMS[3] data acquired using any combination of HCD and CID. The
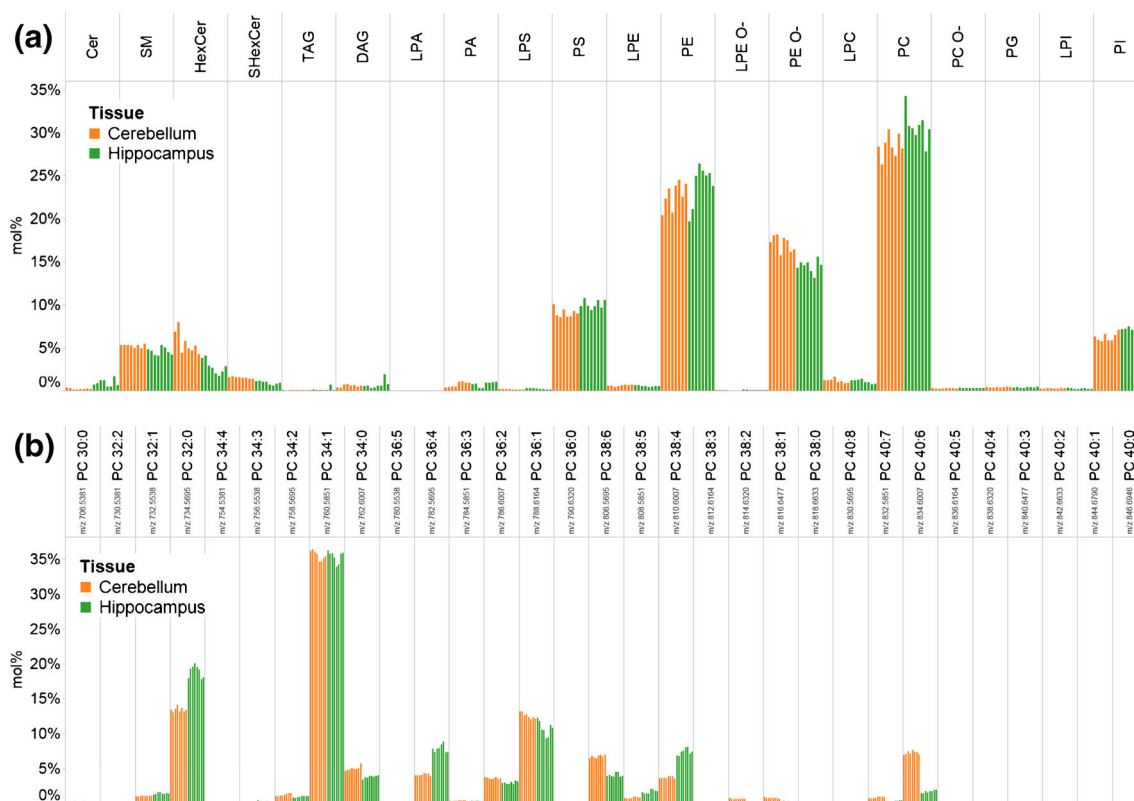
Figure 5. Lipid composition of mouse cerebellum and hippocampus determined using the MS^{ALL} method. (**a**) Lipid class composition. (**b**) PC species composition. Lipid species are annotated by sum composition. Data for 16 sample injections are displayed in order to show the reproducibility obtained using the Orbitrap Fusion-based platform. The 16 samples include four biological replicates of mouse cerebellum and hippocampus, each sample analyzed by two replicate injections. Data are displayed in the same order as in Figure S3 in Supporting Information

ALEX^{123} was designed to compile output data in database table format [32], which allows tracking all experimental data across large sample sets (e.g., polarity, ion activation, ion detection, measured *m/z* values of all fragment ion across all samples) and subsequent data filtering, quality control, and visualization using Tableau Desktop (Figure 5 and S3 in Supporting Information).

To evaluate the efficacy of the MS^{ALL} approach for identification of molecular glycerophospholipid species, we queried FTMS^2 and ITMS^3 data of the 32 samples of mouse cerebellum and hippocampus. For each mode of polarity, we performed searches for identifying molecular glycerophospholipid species detected by FTMS^2 using HCD, FTMS^2 using CID, and ITMS^3 using CID-CID. Next, we included a series of quality control filters to ensure the fidelity of lipid identifications. These included intensity filtering (see Section 2) and the criterion that molecular lipid species should be identified by at least one structure-specific fragment ion in at least half of all sample injections. This criterion was applied separately for each mode of fragmentation analysis. To assess the quality of lipid identification, we compared the number of molecular glycerophospholipid species identified by each mode of fragmentation analysis and counted how many structure-specific fragment ions were detected for each lipid identification (Figure 6a, b). This analysis showed that both positive and negative ion mode FTMS^2 analysis with HCD afforded

identification of more molecular glycerophospholipid species than both FTMS^2 analysis with CID and ITMS^3 analysis. For example, negative ion mode FTMS^2 analysis with HCD allowed identification of 1296 putative molecular lipid species based solely on detection of one structure-specific fragment ion (Figure 6a). We argue that identification of 1296 molecular glycerophospholipid species in mouse brain is an unrealistic number given that only 183 glycerophospholipid species were detected by high resolution FTMS analysis and annotated by sum composition. Moreover, the majority of identified molecular lipid species featured a composition of fatty acid moieties that are difficult to ascribe to brain lipid metabolism. In comparison, the number of molecular glycerophospholipid species identified by negative ion mode FTMS^2 analysis with HCD and detected by three or more fragment ions was only 163 (Figure 6c), a more realistic number of molecular glycerophospholipid species. In addition, the majority of these shortlisted molecular lipid species can be explained by lipid metabolic pathways. We note that similar results were observed for molecular lipid species identified by fragmentation analysis in positive ion mode (Figure 6d). Importantly, the number of molecular glycerophospholipid species identified by positive ion mode FTMS^2 analysis with HCD and detected by three or more structure-specific fragment ions was 35. Interestingly, the analysis of lipid identifications demonstrated that certain
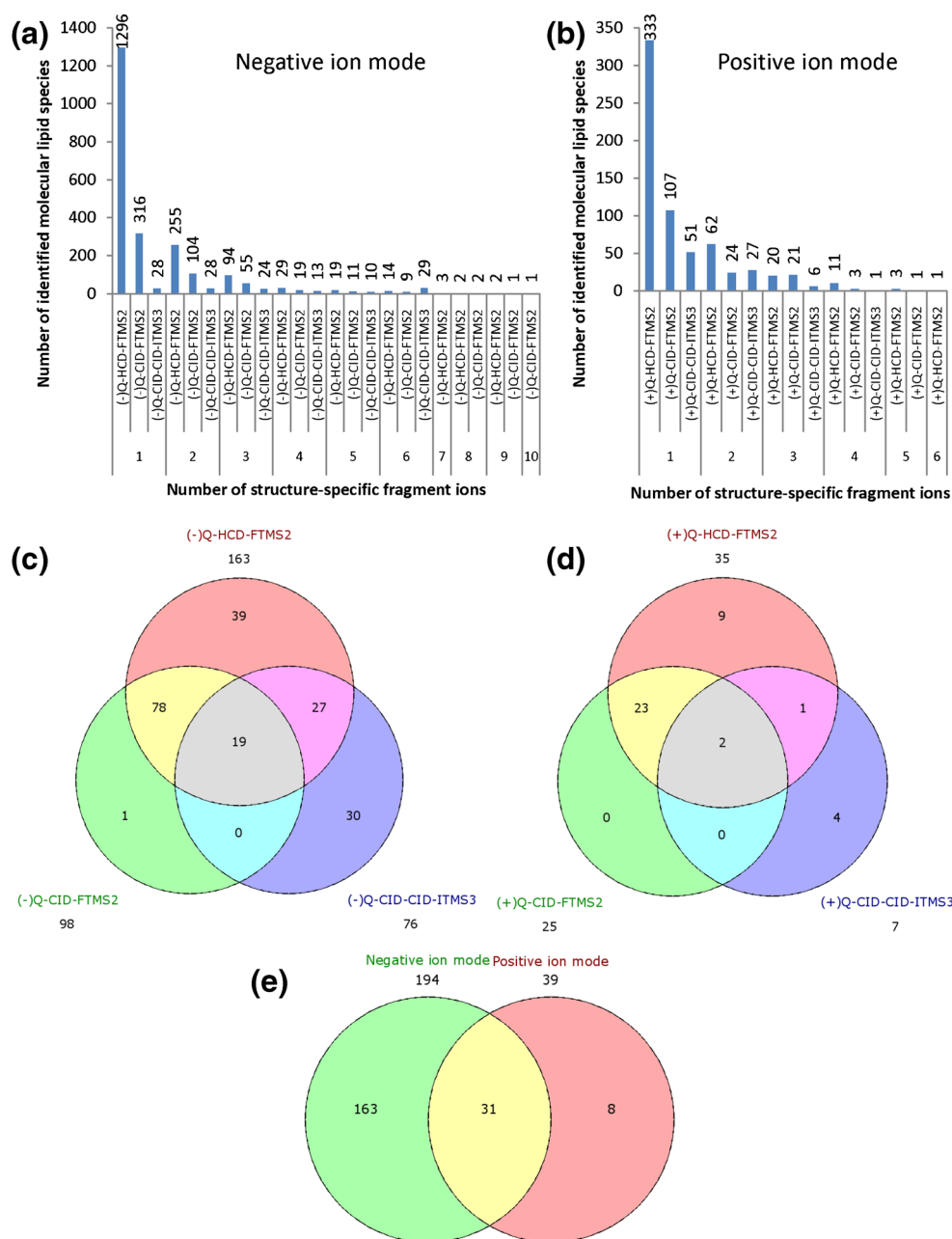
Figure 6. Identification of molecular glycerophospholipid species by MS^{ALL}. (**a**) Number of molecular glycerophospholipid species identified in negative ion mode as a function of mode of fragmentation analysis and number of detected structure-specific fragment ions. (**b**) Number of molecular glycerophospholipid species identified in positive ion mode as a function of mode of fragmentation analysis and number of detected structure-specific fragment ions. (**c**) Venn diagram of molecular glycerophospholipid species identified in negative ion mode by at least three structure-specific fragment ions. (**d**) Venn diagram of molecular glycerophospholipid species identified in positive ion mode by at least three structure-specific fragment ions. (**e**) Venn diagram of molecular lipid species identified in both negative and by positive ion mode by at least three structure-specific fragment ions. For all identifications, it was required that the molecular glycerophospholipid species were identified in at least half of all sample injections. Molecular glycerophospholipid species counted in Venn diagrams are listed in Table S1 in Supporting Information

molecular lipid species in negative and positive ion mode could be detected with up to 10 and six structure-specific fragment ions, respectively (Figure 6a, b). This result demonstrates the efficacy of the MS^{ALL} method for lipid identification and detection of multiple structure-specific fragment ions with high mass resolution and high mass accuracy. Moreover, manual

inspection of shortlisted molecular lipid species demonstrated that high confidence identification requires detection of three or more molecular structure-specific fragment ions.

To further interrogate the efficacy of lipid identification, we applied the criterion that molecular glycerophospholipid species should be detected by at least three structure-specific

fragment ions in at least half of all sample injections. We then compared the shortlists of molecular glycerophospholipid species identified by FTMS^2 analysis using HCD, FTMS^2 analysis using CID, and ITMS^3 analysis. This evaluation demonstrated that all modes of negative ion fragmentation analysis collectively identified 194 molecular glycerophospholipid species (Table S1 in Supporting Information). Nineteen lipid species were identified by all modes of analysis. Moreover, FTMS^2 with HCD afforded identification of all molecular lipid species identified by FTMS^2 analysis using CID, expect for one lipid species. Comparison of negative ion mode FTMS^2 with HCD and ITMS^3 analysis showed an overlap of 46 lipid species and the unique detection of 30 molecular lipid species identified by ITMS^3 (Figure 6c). Importantly, this result demonstrates the efficacy of implementing the complementary ITMS^3 routine for in-depth structural analysis. Notably, the majority of unique lipid species identified using ITMS^3 were PS and PC species. For example, the species PS 16:0-22:6 was, on average, detected by 5, 3, and 6 structure-specific fragment ions by negative ion mode FTMS^2 with HCD, FTMS^2 with CID, and ITMS^3 analysis, respectively (Figure S3 in Supporting Information). Similar results were obtained by comparison of molecular lipid species identified by positive ion mode FTMS^2 and ITMS^3 analysis (Figure 6d). Finally, we compared the number of molecular glycerophospholipid species identified by all modes of fragmentation in negative and positive ion mode (Figure 6e). This analysis demonstrated the collective identification of 202 molecular glycerophospholipid species. Thirty-one lipid species were identified by both positive and negative ion mode analysis, whereas eight and 163 lipid species were identified by positive and negative ion mode fragmentation analysis, respectively. The higher number of identified molecular glycerophospholipid species in negative ion mode is explained by (1) the preferential ionization of majority of glycerophospholipids [3], and (2) the higher relative intensity of structure-specific fragment ions in this mode of analysis. Based on these results, we conclude that the MS^{ALL} method successfully affords comprehensive lipidome analysis. We note that the number of identified molecular species can in the future be increased by expanding the lipid fragmentation database with detailed fragmentation patterns of molecular sphingolipid, glycerolipid, lysoglycerophospholipid, and sterol lipid species, and repeating searches and analysis of the acquired data.

Conclusions

Here, we evaluated the performance of a novel lipidomics platform featuring an Orbitrap Fusion equipped with an automated Triversa Nanomate nanoelectrospray ion source. We demonstrate that the platform affords specific detection of isotopologues of distinct lipid species with high isotope fidelity and features a linear dynamic quantification range of at least four orders of magnitude. Furthermore, we show that

combinatorial fragmentation analysis by multistage activation using both HCD and CID ion activation supports high confidence identification of molecular lipid species. To validate the performance of the platform for in-depth lipidome analysis, we developed an MS^{ALL} method and performed a comparative analysis of mouse cerebellum and hippocampus. This approach afforded absolute quantification of 311 lipid species belonging to 20 lipid classes by high resolution FTMS analysis, and in-depth molecular characterization of 202 distinct molecular glycerophospholipid species using FTMS^2 and ITMS^3 analysis combined with a new filtering strategy for high fidelity lipid identification. Based on our systematic evaluations, we conclude that the Orbitrap Fusion-based platform and the MS^{ALL} approach is a powerful new resource for in-depth lipidome analysis. We note, however, that future improvements are required for unleashing the full potential of the Orbitrap Fusion for comprehensive lipidome analysis. This includes improvements of the acquisition software for supporting DDA-based MS^3 analysis triggered by DIA-based MS^2 data, and providing control of ion trap activation Q parameter for supporting detection of low range *m/z* fragment ions by CID (e.g., the PC-specific fragment ion with *m/z* 184.0733). Furthermore, new and more extensive lipid fragmentation databases should be compiled with information on low abundant molecular structure-specific fragment ions and fragmentation patterns detectable by multidimensional MS^n analysis [51], and as well implementation of new algorithms using combinations of high resolution and all MS^{ALL} data for supporting high confidence lipid identification. For example, in-depth structural analysis of lipid species with more than two fatty acid moieties, such as TAG species, requires detailed characterization of MS^n fragmentation patterns using CID and HCD as well as compiling a comprehensive lipid database and designing an identification routine that supports high confidence identification. Importantly, our results demonstrate that high confidence identification of molecular lipid species detected by high resolution FTMS should be based on detection of at least three structure-specific fragment ions. Finally, we note that the Orbitrap Fusion also supports high scan speed FTMS acquisitions (up to 30 Hz), which provide an analytical avenue for the development of new high resolution LC-MS-MS^n-based lipidomic workflows.

Acknowledgments

References

1. Shevchenko, A., Simons, K.: Lipidomics: coming to grips with lipid diversity. Nat. Rev. Mol. Cell Biol. **11**, 593–598 (2010)
2. van Meer, G.: Cellular lipidomics. EMBO J. **24**, 3159–3165 (2005)
3. Ejsing, C.S., Sampaio, J.L., Surendranath, V., Duchoslav, E., Ekroos, K., Klemm, R.W., Simons, K., Shevchenko, A.: Global analysis of the yeast lipidome by quantitative shotgun mass spectrometry. Proc. Natl. Acad. Sci. U. S. A. **106**, 2136–2141 (2009)
4. Fahy, E., Subramaniam, S., Brown, H.A., Glass, C.K., Merrill Jr., A.H., Murphy, R.C., Raetz, C.R., Russell, D.W., Seyama, Y., Shaw, W., Shimizu, T., Spener, F., van Meer, G., VanNieuwenhze, M.S., White, S.H., Witztum, J.L., Dennis, E.A.: A comprehensive classification system for lipids. J. Lipid Res. **46**, 839–861 (2005)
5. Wymann, M.P., Schneiter, R.: Lipid signalling in disease. Nat. Rev. Mol. Cell Biol. **9**, 162–176 (2008)
6. Klose, C., Surma, M.A., Gerl, M.J., Meyenhofer, F., Shevchenko, A., Simons, K.: Flexibility of a eukaryotic lipidome—insights from yeast lipidomics. PLoS One **7**, e35063 (2012)
7. Carvalho, M., Sampaio, J.L., Palm, W., Brankatschk, M., Eaton, S., Shevchenko, A.: Effects of diet and development on the Drosophila lipidome. Mol. Syst. Biol. **8**, 600 (2012)
8. Dennis, E.A., Deems, R.A., Harkewicz, R., Quehenberger, O., Brown, H.A., Milne, S.B., Myers, D.S., Glass, C.K., Hardiman, G., Reichart, D., Merrill Jr., A.H., Sullards, M.C., Wang, E., Murphy, R.C., Raetz, C.R., Garrett, T.A., Guan, Z., Ryan, A.C., Russell, D.W., McDonald, J.G., Thompson, B.M., Shaw, W.A., Sud, M., Zhao, Y., Gupta, S., Maurya, M.R., Fahy, E., Subramaniam, S.: A mouse macrophage lipidome. J. Biol. Chem. **285**, 39976–39985 (2010)
9. Tarasov, K., Ekroos, K., Suoniemi, M., Kauhanen, D., Sylvanne, T., Hurme, R., Gouni-Berthold, I., Berthold, H.K., Kleber, M.E., Laaksonen, R., Marz, W.: Molecular lipids identify cardiovascular risk and are efficiently lowered by simvastatin and PCSK9 deficiency. J. Clin. Endocrinol. Metab. **99**, E45–E52 (2014)
10. Han, X., Yang, K., Gross, R.W.: Multi-dimensional mass spectrometry-based shotgun lipidomics and novel strategies for lipidomic analyses. Mass Spectrom. Rev. **31**, 134–178 (2012)
11. Harkewicz, R., Dennis, E.A.: Applications of mass spectrometry to lipids and membranes. Annu. Rev. Biochem. **80**, 301–325 (2011)
12. Blanksby, S.J., Mitchell, T.W.: Advances in mass spectrometry for lipidomics. Annu. Rev. Anal. Chem. (Palo Alto, CA) **3**, 433–465 (2010)
13. Serhan, C.N.: Mediator lipidomics. Prostaglandins Other Lipid Mediat. **77**, 4–14 (2005)
14. Ekroos, K., Chernushevich, I.V., Simons, K., Shevchenko, A.: Quantitative profiling of phospholipids by multiple precursor ion scanning on a hybrid quadrupole time-of-flight mass spectrometer. Anal. Chem. **74**, 941–949 (2002)
15. Simons, B., Kauhanen, D., Sylvanne, T., Tarasov, K., Duchoslav, E., Ekroos, K.: Shotgun lipidomics by sequential precursor ion fragmentation on a hybrid quadrupole time-of-flight mass spectrometer. Metabolites **2**, 195–213 (2012)
16. Schwudke, D., Hannich, J.T., Surendranath, V., Grimard, V., Moehring, T., Burton, L., Kurzchalia, T., Shevchenko, A.: Top-down lipidomic screens by multivariate analysis of high-resolution survey mass spectra. Anal. Chem. **79**, 4083–4093 (2007)
17. Fauland, A., Kofeler, H., Trotzmuller, M., Knopf, A., Hartler, J., Eberl, A., Chitraju, C., Lankmayr, E., Spener, F.: A comprehensive method for lipid profiling by liquid chromatography-ion cyclotron resonance mass spectrometry. J. Lipid Res. **52**, 2314–2322 (2011)
18. Liebisch, G., Vizcaino, J.A., Kofeler, H., Trotzmuller, M., Griffiths, W.J., Schmitz, G., Spener, F., Wakelam, M.J.: Shorthand notation for lipid structures derived from mass spectrometry. J. Lipid Res. **54**, 1523–1530 (2013)
19. Ejsing, C.S., Husen, P., Tarasov, K.: In: Ekroos, K. (ed.) Lipidomics: Technologies and Applications, pp. 147–174. Wiley-VCH, Weinheim (2012)
20. Foster, J.M., Moreno, P., Fabregat, A., Hermjakob, H., Steinbeck, C., Apweiler, R., Wakelam, M.J., Vizcaino, J.A.: LipidHome: a database of theoretical lipids optimized for high throughput mass spectrometry lipidomics. PLoS One **8**, e61951 (2013)
21. Ekroos, K., Ejsing, C.S., Bahr, U., Karas, M., Simons, K., Shevchenko, A.: Charting molecular composition of phosphatidylcholines by fatty acid scanning and ion trap MS3 fragmentation. J. Lipid Res. **44**, 2181–2192 (2003)
22. Thomas, M.C., Mitchell, T.W., Harman, D.G., Deeley, J.M., Nealon, J.R., Blanksby, S.J.: Ozone-induced dissociation: elucidation of double bond position within mass-selected lipid ions. Anal. Chem. **80**, 303–311 (2008)
23. Pham, H.T., Maccarone, A.T., Thomas, M.C., Campbell, J.L., Mitchell, T.W., Blanksby, S.J.: Structural characterization of glycerophospholipids by combinations of ozone- and collision-induced dissociation mass spectrometry: the next step towards "top-down" lipidomics. Analyst **139**, 204–214 (2014)
24. Maccarone A.T., Duldig J., Mitchell T.W., Blanksby S.J., Duchoslav E., Campbell J.L.: Rapid and unambiguous characterization of acyl chain position in unsaturated phosphatidylcholines using differential mobility and mass spectrometry. J. Lipid Res **55**, 1668–1677 (2014)
25. Scigelova M., Hornshaw M., Giannakopulos A., Makarov A.: Fourier transform mass spectrometry. Mol. Cell. Proteom **10**, M111. 009431 (2011)
26. Li, F., Qin, X., Chen, H., Qiu, L., Guo, Y., Liu, H., Chen, G., Song, G., Wang, X., Li, F., Guo, S., Wang, B., Li, Z.: Lipid profiling for early diagnosis and progression of colorectal cancer using direct-infusion electrospray ionization Fourier transform ion cyclotron resonance mass spectrometry. Rapid Commun. Mass Spectrom. **27**, 24–34 (2013)
27. Lane, A.N., Fan, T.W., Xie, Z., Moseley, H.N., Higashi, R.M.: Isotopomer analysis of lipid biosynthesis by high resolution mass spectrometry and NMR. Anal. Chim. Acta. **651**, 201–208 (2009)
28. Yang, H.J., Park, K.H., Lim, D.W., Kim, H.S., Kim, J.: Analysis of cancer cell lipids using matrix-assisted laser desorption/ionization 15-T Fourier transform ion cyclotron resonance mass spectrometry. Rapid Commun. Mass Spectrom. **26**, 621–630 (2012)
29. Zech, T., Ejsing, C.S., Gaus, K., de Wet, B., Shevchenko, A., Simons, K., Harder, T.: Accumulation of raft lipids in T-cell plasma membrane domains engaged in TCR signalling. EMBO J. **28**, 466–476 (2009)
30. Sampaio, J.L., Gerl, M.J., Klose, C., Ejsing, C.S., Beug, H., Simons, K., Shevchenko, A.: Membrane lipidome of an epithelial cell line. Proc. Natl. Acad. Sci. U. S. A. **108**, 1903–1907 (2011)
31. Ejsing, C.S., Moehring, T., Bahr, U., Duchoslav, E., Karas, M., Simons, K., Shevchenko, A.: Collision-induced dissociation pathways of yeast sphingolipids and their molecular profiling in total lipid extracts: a study by quadrupole TOF and linear ion trap-Orbitrap mass spectrometry. J. Mass Spectrom. **41**, 372–389 (2006)
32. Husen, P., Tarasov, K., Katafiasz, M., Sokol, E., Vogt, J., Baumgart, J., Nitsch, R., Ekroos, K., Ejsing, C.S.: Analysis of lipid experiments (ALEX): a software framework for analysis of high-resolution shotgun lipidomics data. PLoS One **8**, e79736 (2013)
33. Han, X., Gross, R.W.: Shotgun lipidomics: electrospray ionization mass spectrometric analysis and quantitation of cellular lipidomes directly from crude extracts of biological samples. Mass Spectrom. Rev. **24**, 367–412 (2005)
34. Ejsing, C.S., Duchoslav, E., Sampaio, J., Simons, K., Bonner, R., Thiele, C., Ekroos, K., Shevchenko, A.: Automated identification and quantification of glycerophospholipid molecular species by multiple precursor ion scanning. Anal. Chem. **78**, 6202–6214 (2006)
35. Erve, J.C., Gu, M., Wang, Y., DeMaio, W., Talaat, R.E.: Spectral accuracy of molecular ions in an LTQ/Orbitrap mass spectrometer and implications for elemental composition determination. J. Am. Soc. Mass Spectrom. **20**, 2058–2069 (2009)
36. Kaufmann, A., Walker, S.: Accuracy of relative isotopic abundance and mass measurements in a single-stage Orbitrap mass spectrometer. Rapid Commun. Mass Spectrom. **26**, 1081–1090 (2012)
37. Randall, S.M., Cardasis, H.L., Muddiman, D.C.: Factorial experimental designs elucidate significant variables affecting data acquisition on a quadrupole orbitrap mass spectrometer. J. Am. Soc. Mass Spectrom. **24**, 1501–1512 (2013)
38. Vining, B.A., Bossio, R.E., Marshall, A.G.: Phase correction for collision model analysis and enhanced resolving power of fourier transform ion cyclotron resonance mass spectra. Anal. Chem. **71**, 460–467 (1999)
39. Stahlman, M., Ejsing, C.S., Tarasov, K., Perman, J., Boren, J., Ekroos, K.: High-throughput shotgun lipidomics by quadrupole time-of-flight mass

spectrometry. J. Chromatogr. B Analyt. Technol. Biomed. Life Sci. **877**, 2664–2672 (2009)

40. Hsu, F.F., Turk, J.: Studies on phosphatidylserine by tandem quadrupole and multiple stage quadrupole ion-trap mass spectrometry with electrospray ionization: structural characterization and the fragmentation processes. J. Am. Soc. Mass Spectrom. **16**, 1510–1522 (2005)

41. Hsu, F.F., Turk, J.: Electrospray ionization/tandem quadrupole mass spectrometric studies on phosphatidylcholines: the fragmentation processes. J. Am. Soc. Mass Spectrom. **14**, 352–363 (2003)

42. Hsu, F.F., Turk, J.: Characterization of phosphatidylinositol, phosphatidylinositol-4-phosphate, and phosphatidylinositol-4,5-bisphosphate by electrospray ionization tandem mass spectrometry: a mechanistic study. J. Am. Soc. Mass Spectrom. **11**, 986–999 (2000)

43. Hsu, F.F., Turk, J.: Charge-remote and charge-driven fragmentation processes in diacyl glycerophosphoethanolamine upon low-energy collisional activation: a mechanistic proposal. J. Am. Soc. Mass Spectrom. **11**, 892–899 (2000)

44. Hsu, F.F., Turk, J.: Charge-driven fragmentation processes in diacyl glycerophosphatidic acids upon low-energy collisional activation. A mechanistic proposal. J. Am. Soc. Mass Spectrom. **11**, 797–803 (2000)

45. Hsu, F.F., Turk, J.: Characterization of ceramides by low energy collisional-activated dissociation tandem mass spectrometry with negative-ion electrospray ionization. J. Am. Soc. Mass Spectrom. **13**, 558–570 (2002)

46. Pulfer, M., Murphy, R.C.: Electrospray mass spectrometry of phospholipids. Mass Spectrom. Rev. **22**, 332–364 (2003)

47. Sokol, E., Almeida, R., Hannibal-Bach, H.K., Kotowska, D., Vogt, J., Baumgart, J., Kristiansen, K., Nitsch, R., Knudsen, J., Ejsing, C.S.: Profiling of lipid species by normal-phase liquid chromatography, nanoelectrospray ionization, and ion trap-orbitrap mass spectrometry. Anal. Biochem. **443**, 88–96 (2013)

48. Southam, A.D., Payne, T.G., Cooper, H.J., Arvanitis, T.N., Viant, M.R.: Dynamic range and mass accuracy of wide-scan direct infusion nanoelectrospray Fourier transform ion cyclotron resonance mass spectrometry-based metabolomics increased by the spectral stitching method. Anal. Chem. **79**, 4595–4602 (2007)

49. Curk, T., Demsar, J., Xu, Q., Leban, G., Petrovic, U., Bratko, I., Shaulsky, G., Zupan, B.: Microarray data mining with visual programming. Bioinformatics **21**, 396–398 (2005)

50. Chan, R.B., Oliveira, T.G., Cortes, E.P., Honig, L.S., Duff, K.E., Small, S.A., Wenk, M.R., Shui, G., Di Paolo, G.: Comparative lipidomic analysis of mouse and human brain with Alzheimer disease. J. Biol. Chem. **287**, 2678–2688 (2012)

51. Hsu F.F., Lodhi I.J., Turk J., Semenkovich C.F.: Structural distinction of diacyl-, alkylacyl, and alk-1-enylacyl glycerophosphocholines as [M − 15] ions by multiple-stage linear ion-trap mass spectrometry with electrospray ionization. J. Am. Soc. Mass Spectrom **25**, 1412-1420 (2014)